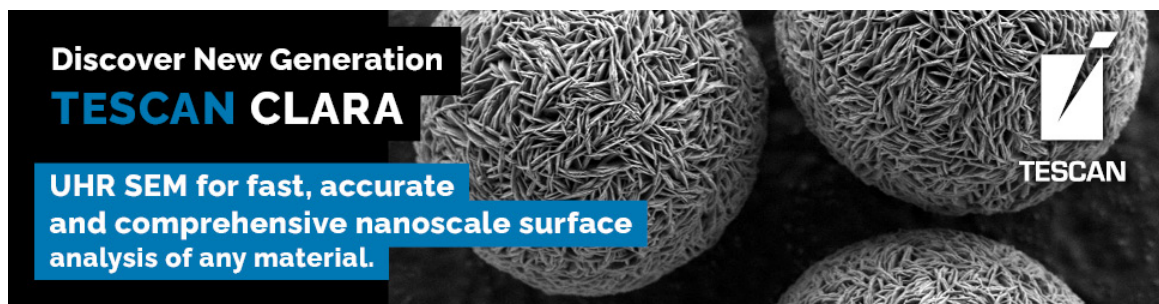



Thickness-Dependent Layer Stacking Disorder in Low and High Temperature Phase of MoTe₂ via STEM Imaging

Lopa Bhatt, James L Hart, Elisabeth Bianco, Judy Cha, Lena F Kourkoutis



Discover New Generation
TESCAN CLARA

UHR SEM for fast, accurate
and comprehensive nanoscale surface
analysis of any material.



TESCAN

Meeting-report

Thickness-Dependent Layer Stacking Disorder in Low and High Temperature Phase of MoTe₂ via STEM Imaging

Lopa Bhatt¹, James L. Hart², Elisabeth Bianco³, Judy Cha², and Lena F. Kourkoutis^{1,3,*}

¹School of Applied and Engineering Physics, Cornell University, Ithaca, NY, United States

²Department of Materials Science and Engineering, Cornell University, Ithaca, NY, United States

³Kavli Institute at Cornell for Nanoscale Science, Cornell University, Ithaca, NY, United States

*Corresponding author: lena.f.kourkoutis@cornell.edu

Properties of layered two-dimensional (2D) materials such as the band gap and ferroelectricity can be controlled by engineering their layer stacking for promising applications in quantum transport devices, energy materials and optical components [1,2]. For instance, small shifts in the layer-stacking order alone transform MoTe₂, a 2D transition metal dichalcogenide (TMD), from the higher order topological insulator 1T' phase to the Weyl semimetal T_d phase [3]. This phase transition from the monoclinic 1T' to the orthorhombic T_d structure occurs upon cooling bulk 1T' below ~250 K. [3]. Due to the weak out of plane van der Waals bonding, MoTe₂ is very susceptible to stacking disorder which can drastically alter and suppress the phase transition [4]. Hence, precise characterization of these layer stacking disorders is critical to understanding the phase transition.

In principle, the evolution of the layer stacking order in MoTe₂ through the 1T'-T_d transition can be directly probed in real space at atomic resolution with cross-sectional cryogenic scanning transmission electron microscope (STEM) imaging [5]. In-plane confinement imposed by the cross-sectional TEM lamella geometry, however, suppresses the phase transition likely due to modifications of the surface of the TEM lamella during the focused ion beam (FIB) process. Here, we overcome this limitation by a combination of cryogenic plan-view STEM imaging and room-temperature cross-sectional STEM imaging to study layer stacking and disorder. Insight from these two complementary techniques allow us to measure the structure of MoTe₂ at atomic resolution on both side of the phase transition, finding significant layer stacking disorder and characterizing its dependence on thickness in MoTe₂.

Flakes of MoTe₂ were exfoliated over holes on a silicon nitride TEM grid for plan-view (*ab-plane*) imaging with a Gatan 636 double-tilt cryogenic sample holder. Plan-view samples were imaged at room temperature (~300 K) and liquid nitrogen temperature (~100 K) revealing strikingly different atomic arrangements on either side of the 1T'-T_d transition (Fig. 1a, b). Additionally, in different areas of the flake, several different configurations were measured at each temperature, indicating an inhomogeneous structure consistent with layer stacking disorder along the projection direction. Multislice image simulations [6] of the 1T' and T_d phases (Fig. 1c) do not match any of the experimental images further indicating presence of disorder. To explain these structural variations seen in the plan-view images, cross-sectional study of MoTe₂ was performed.

Cross-sectional lamellae of MoTe₂ were prepared by FIB lift out. The lamellas were imaged in the *ac-plane* of MoTe₂ flakes (Fig. 2b-d). As discussed previously, the 1T' and T_d phases are differentiated by their layer stacking order, which can be directly identified by measuring the direction of interlayer Te-Te displacement as shown in Fig. 2a. The directions were obtained by fitting every Te column with a 6 parameter 2D Gaussian and averaging over the Te-Te displacements between each layer. In agreement with the plan-view images, layer stacking disorder, indicated by irregular flips of the arrow directions in Fig. 2b-d, was observed in all measured flakes at room temperature. Surprisingly, the extent of layer stacking disorder was found to decrease with the thickness of the flake (Fig. 2b-d). Bulk flakes were found to have infrequent twin stacking faults separated by over 15 layers, while intermediate thickness flakes on the order of ~40 nm had twin stacking faults separated by less than 10 layers. In even thinner flakes (~10nm), remarkably, stabilization of few layers of T_d structure was observed along with densely packed 1T' twin faults. The thickness dependent disorder can explain the inhomogeneity present in the plan-view STEM imaging of exfoliated flakes which are not of uniform thickness. Understanding this layer stacking disorder in MoTe₂ through the 1T'-T_d phase transition and as a function of thickness is crucial for its applications. Combining plan-view and cross-sectional STEM imaging has provided a way to strengthen our understanding of layer stacking and disorder in 2D materials [7].

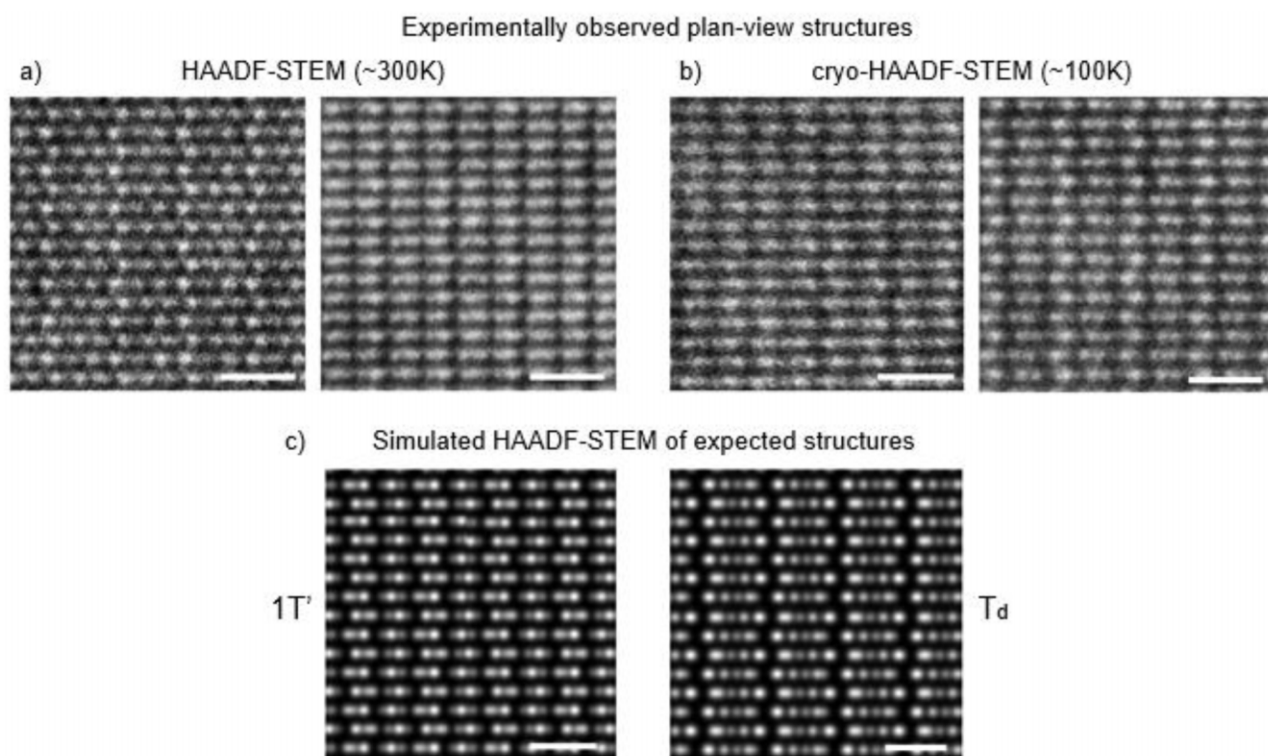


Fig. 1. Various structures observed in plan-view (ab-plane) HAADF-STEM images of MoTe₂ flakes at a) room temperature (~300 K) and b) at liquid nitrogen temperature (~100 K). c) Multislice simulations of 3 layers of 1T' and 4 layers of T_d MoTe₂ in plan-view show that the experimentally observed structures are distinct from the pure 1T' and T_d phases of MoTe₂. All scale bars correspond to 7Å.

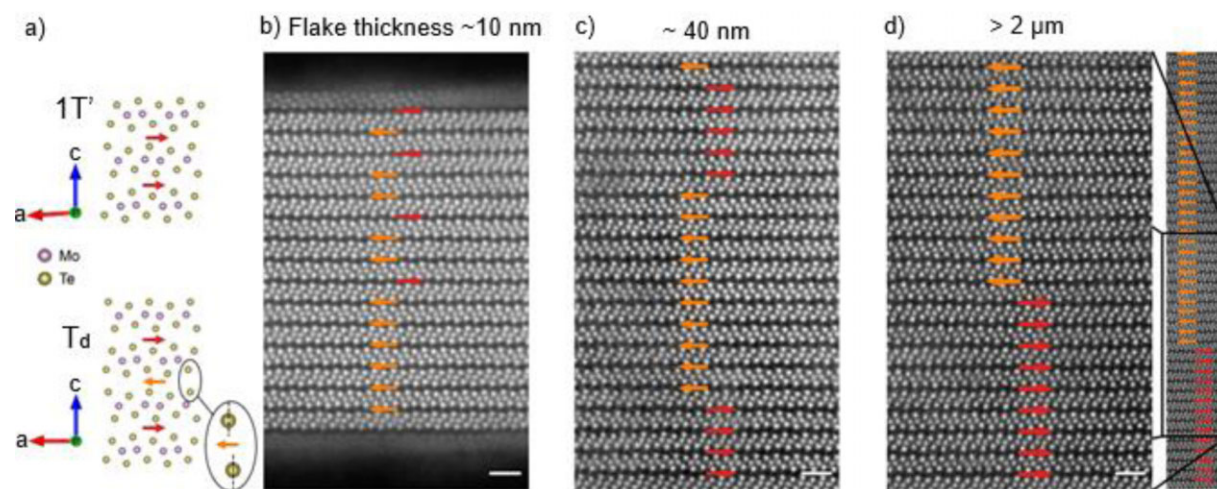


Fig. 2. a) Schematic of the 1T' and T_d phases of MoTe₂ in cross-section (ac-plane) with arrows depicting the direction of interlayer Te-Te displacements. Thickness dependent disorder observed in cross-sectional HAADF-STEM images of (b) ~10 nm thick, (c) ~40 nm thick and (d) bulk (>2 μm) MoTe₂. All the scale bars correspond to 1 nm.

References

1. W Bao *et al.*, *Nature Physics* 7 (2011), p.948. doi:10.1038/nphys2103
2. K Yasuda *et al.*, *Science* 372 (2021), p.1458. doi:10.1126/science.abd3230
3. Y Deng *et al.*, *ACS Nano* 15 (2021), p.12465. doi:10.1021/acsnano.1c01816
4. Y Cheon *et al.*, *ACS Nano* 15 (2021), p. 2962. doi:10.1021/acsnano.0c09162
5. I El Baggari *et al.* *PNAS* 115 (2017), p. 1445. doi:10.1073/pnas.1714901115
6. EJ Kirkland, “*Advanced Computing in Electron Microscopy*”, Springer (US, Boston, MA), 2010
7. This work made use of the electron microscopy facility of the Platform for the Accelerated Realization, Analysis, and Discovery of Interface Materials (PARADIM), which is supported by the National Science Foundation under Cooperative Agreement No. DMR-2039380, and the Cornell Center for Materials Research Shared Facilities which are supported through the NSF MRSEC program (DMR-1719875).



TESCAN TENSOR

Integrated, Precession-Assisted,
Analytical 4D-STEM



Visit us and learn more
about our TESCAN TENSOR

info.tescan.com/stem